Accurate and Direct Characterization of High-Q Microwave Resonators Using One-Port Measurement

Lye Heng Chua, *Student Member, IEEE,* and Dariush Mirshekar-Syahkal, *Senior Member, IEEE*

***Abstract*—An accurate and direct characterization of high-Q microwave resonators using one-port vector network measurement technique is presented. In this characterization, the delay due to the connector between the resonator and network analyzer is first deembeded. The elements of the equivalent-circuit of the resonator are then readily extracted from the experimental data in a straightforward manner without any numerical optimization. The extraction method works very accurately for high-Q resonators coupled to external circuits electrically or magnetically, and can deal with universal cases including external lossy couplings and weak under-coupled resonators. Parameters such as coupling coefficient, loaded quality factor, and loaded resonant frequency can also be directly computed. For the loaded resonant frequency, an original expression is derived in this paper. This paper also provides an approximate relation between the loaded resonant frequency and measured frequency at which the minimum magnitude of the reflection coefficient occurs. The high accuracy of the method is demonstrated with two examples, a hollow cavity resonator and a dielectric loaded cavity resonator, which is also supported by the well-established one-port multipoint technique.**

***Index Terms*—Critical-points method, high-Q resonator, one-port measurement.**

I. Introduction

MICROWAVE resonators are important circuit components for devices like filters, multipliers, and oscillators. As such, a fast and accurate characterization of the resonator is essential in assisting circuit designers to accurately predict the performance of any microwave circuit in which the resonator is used. Three important parameters associated with a resonator are the resonator unloaded Q factor (Q_o), the coupling coefficient (κ), and the loaded resonant frequency (f_L). The unloaded Q factor establishes an upper limit on the resonator performance, while the coupling coefficient κ describes how the resonator interacts with microwave circuits interfaced with the resonator. The loaded resonant frequency (f_L), on the other hand, represents the shift of frequency from its natural resonant frequency (f_o) when it is coupled to the external circuit.

A vast number of publications have been reported on the characterization of the resonator Q factors [1]–[12]. Ginzton [1] and Podcameni *et al*. [2] had devised a graphical method to determine the resonator Q factors, which was further developed and used by Khanna and Garault [3] in the computation of the Q factors of a dielectric resonator coupled to a microstrip line. However, such an approach requires the construction of a linear frequency scale or the $R = \pm jX$ arcs on the Smith chart, superimposed with the resonator measured reflection coefficient locus in order to determine the Q factors of the resonator.

The advent of sophisticated network analyzers has allowed the introduction of a one-port reflection technique [4]–[11] and two-port transmission technique [5]–[8], [12]–[15] of characterizing resonator Q factors. In most of these publications, either an overly simplified equivalent circuit has been adopted [6]–[8] or the least-square curve-fitting procedure to the measured data [4], [5], [9], [13], [14] has been used. In the two-port transmission method of the Q-factor measurement, the error in the unloaded Q factor could be large (above 10%) due to the inequality of the input and output coupling coefficients and the effect of coupling losses and, hence, as a rule-of-thumb, it is not recommended for overcoupled resonators [15].

In one case, Kwok and Liang [10] has presented a one-port reflection technique of characterizing the unloaded Q factor using the scalar network analyzer with the help of a lookup table or plot. However, such a technique requires special arrangement of the input coupling in order to meet certain criterion. Also, an additional experimental verification is needed in order to decide whether the measured data is for the overcoupled or undercoupled case. On the other hand, the one-port technique, the critical-points method, developed by Sun and Chao [11], is fast and accurate for the measurement of the unloaded Q. Only four frequencies are needed from which the unloaded Q factor is accurately computed from the measured one-port input reflection coefficient.

In this paper, we extend the work of Sun and Chao [11] to directly extract all the elements of an equivalent circuit used to describe a high-Q microwave resonator and its coupling elements to the external circuit including the delay due to the connector. The equivalent circuit of the resonator is extremely useful since it can be employed in any circuit simulator, such as the Advanced Design System (ADS),[1] for accurate prediction of the performance of a microwave filter based on the resonator [16], or it can be used for computer-controlled automated tuning of microwave filters [17], [18]. From the equivalent circuit, the unloaded Q factor, coupling coefficient, and loaded resonant frequency can be directly computed. For the loaded resonant frequency, an original expression is derived in this paper, and an approximate relation between the loaded resonant frequency and the frequency at which the minimum magnitude of the reflection coefficient occurs, is given. To illustrate the accuracy

Manuscript received May 15, 2002; revised October 25, 2002.

The authors are with the Department of Electronic Systems Engineering, University of Essex, Colchester CO4 3SQ, U.K.

Digital Object Identifier 10.1109/TMTT.2003.808711

[1]*Advanced Design System*, ver. 1.5, Agilent Technol., Palo Alto, CA.

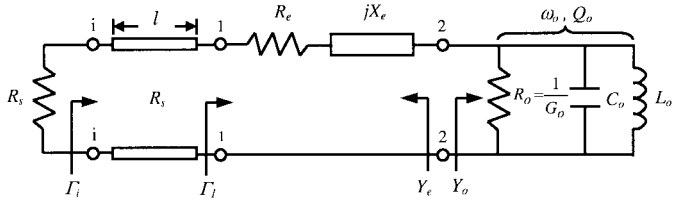

Fig. 1. Equivalent circuit of a high-Q resonator including coupling losses and a transmission line with characteristic impedance R_s.

of the method, the measurement results on two types of resonators, namely, a hollow cavity resonator and a dielectric loaded cavity resonator, are presented and their equivalent circuits are extracted. The high accuracy of the equivalent circuits, the Q factors, and resonant frequencies are supported by the well-established Kajfez's one-port multipoint technique [19] and a circuit simulator software.

II. Equivalent-Circuit Model

It is well known that input impedance of a high-Q resonator can be represented by a an equivalent circuit shown in Fig. 1. In the equivalent circuit, the unloaded resonator is represented by the parallel resonant circuit, characterized by the unloaded resonant angular frequency ω_o, unloaded Q factor Q_o, and resistance R_o, which stands for power dissipation within the unloaded resonator. The external loading circuit is represented by the resistance R_s (typically 50 Ω for a network analyzer) and a section of the transmission line of characteristic impedance R_s connecting the resonator to the network analyzer. The coupling mechanism is characterized by an impedance $R_e + jX_e$. The losses within the coupling mechanism is represented by the resistance R_e, and the extra energy storage introduced by the coupling mechanism is represented by the reactance X_e. The value of the reactance X_e can be positive or negative depending on the coupling mechanism applied. For a small coupling loop, one expects the reactance to be inductive and, hence, $X_e = \omega L_e$, and, for a probe, the reactance should be capacitive and $X_e = -1/\omega C_e$.

The first step for extraction of the circuit elements is to obtain the group delay due to the connecting transmission line (connector length). This can be easily accomplished by measuring the input reflection coefficients of two similar transmission lines of different lengths, say, l_a and l_b, terminated in an identical load at the other end, which could be an open or short circuit. If Γ_t represents the input reflection coefficient of the load, and $\Gamma_{\mathrm{in,a}}$ and $\Gamma_{\mathrm{in,b}}$ represent the corresponding input reflection coefficients with the insertion of the transmission lines at lengths l_a and l_b, respectively, they are then related by the following equations:

$$\Gamma_{\mathrm{in,a}} = e^{-2\gamma l_a}\Gamma_t \tag{1a}$$

$$\Gamma_{\mathrm{in,b}} = e^{-2\gamma l_b}\Gamma_t \tag{1b}$$

where γ is the propagation constant of the transmission line. For low-loss line $\gamma = \alpha + j\beta \approx j\beta$ and, hence, the phase constant can be solved from (1) to give

$$\beta = \frac{-0.5}{l_b - l_a}\mathrm{phase}\left(\frac{\Gamma_{\mathrm{in,b}}}{\Gamma_{\mathrm{in,a}}}\right) = \frac{-0.5}{\Delta l}\mathrm{phase}\left(\frac{\Gamma_{\mathrm{in,b}}}{\Gamma_{\mathrm{in,a}}}\right). \tag{2}$$

The small loss in the transmission line, in this case, is lumped into the R_e in Fig. 1, as part of the losses within the coupling mechanism. Once the phase constant is determined, the effect of delay due to the connector can be deembedded from the measured input reflection coefficient (Γ_i) of the resonator to yield the reflection coefficient at port 1 (Γ_1), as in Fig. 1, which is given by

$$\Gamma_1 = e^{2j\beta l}\Gamma_i. \tag{3}$$

The corresponding input impedance at port 1 can now be represented as follows:

$$\begin{aligned} Z_1(\omega) &= R_e + jX_e + Z_o \\ &= R_e + jX_e + \frac{R_o}{\left(1 + jQ_o\left(\dfrac{\omega}{\omega_o} - \dfrac{\omega_o}{\omega}\right)\right)} \end{aligned} \tag{4a}$$

where

$$\begin{aligned} \omega_o &= \frac{1}{\sqrt{L_o C_o}} \\ Q_o &= \frac{\omega_o C_o}{G_o} = \frac{R_o}{\omega_o L_o} = R_o\sqrt{\frac{C_o}{L_o}} \end{aligned} \tag{4b}$$

and

$$X_e = \begin{cases} \omega L_e & \text{(inductive coupling)} \\ \dfrac{-1}{\omega C_e} & \text{(capacitive coupling).} \end{cases} \tag{4c}$$

For simplicity, the following representation in the vicinity of the natural resonant angular frequency ω_o is used [11]:

$$\frac{\omega_m}{\omega_o} - \frac{\omega_o}{\omega_m} = 2\delta_m \frac{1 + \dfrac{\delta_m}{2}}{1 + \delta_m} = 2\delta_m D_m \approx 2\delta_m, \qquad \text{for } \delta_m \ll 1 \tag{5a}$$

where

$$\delta_m = \frac{\omega_m - \omega_o}{\omega_o} \tag{5b}$$

is the frequency-tuning parameter and

$$D_m = \frac{1 + \dfrac{\delta_m}{2}}{1 + \delta_m} \tag{5c}$$

is the deviation factor of linearity. Plot of a typical impedance locus of $Z_1(\omega)$ is given in Fig. 2. The critical points are marked as ω_1 and ω_2 (i.e., $m = 1, 2$), and the detuned crossover point are indicated as ω_3 and ω_4 (i.e., $m = 3, 4$), respectively, in the plot. Applying the critical-points method of the unloaded Q computation, Q_o can be written as follows [11]:

$$Q_o = \frac{\omega_o}{|\omega_1 - \omega_2|}\,|x| \approx \frac{\omega_o}{|\omega_1 - \omega_2|}, \qquad \text{for } |x| \approx 1 \tag{6a}$$

where

$$\begin{aligned} \omega_o &= \frac{\omega_1 + \omega_2}{2} \\ a &= 2\left(\frac{1}{D_3} + \frac{1}{D_4}\right)^{-1} \\ b &= \left(\frac{\delta_4 D_4 - \delta_3 D_3}{\delta_2 - \delta_1}\right)^2 \end{aligned} \tag{6b}$$

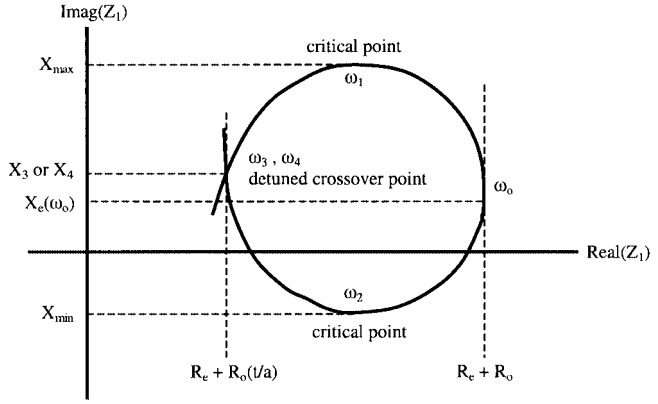

Fig. 2. Input impedance locus of a coupled resonator including coupling losses and reactance in the vicinity of resonant frequency.

and

$$x=\sqrt{\frac{1}{2}\left(\frac{b-2a-1}{a+b}\right)+\sqrt{\frac{1}{4}\left(\frac{b-2a-1}{a+b}\right)^{2}-\frac{a-1}{a+b}}}. \tag{6c}$$

At resonant frequency

$$Z_1(\omega_o)=(R_e+R_o)+jX_e(\omega_o) \tag{7}$$

and at the detuned crossover point (ω_3 and ω_4)

$$Z_1(\omega_3)=Z_1(\omega_4)=\left[R_e+R_o\left(\frac{t}{a}\right)\right]+jX_3 \tag{8a}$$

where

$$t=\frac{a}{1+bx^2} \tag{8b}$$

and

$$X_3=X_4=\begin{cases}\omega_o L_e\left[1+\frac{1}{2}(\delta_3+\delta_4)\right] & \text{(inductive coupling)}\\ -\dfrac{\left[1+\frac{1}{2}(\delta_3+\delta_4)\right]}{\omega_o C_e(1+\delta_3)(1+\delta_4)} & \text{(capacitive coupling).}\end{cases} \tag{8c}$$

From these two equations, R_o, R_e, and L_e or C_e can be determined as follows:

$$R_o=\frac{\text{real}\left[Z_1(\omega_o)-0.5\left(Z_1(\omega_3)+Z_1(\omega_4)\right)\right]}{1-\frac{t}{a}} \tag{9a}$$

$$R_e=\frac{\text{real}\left[0.5\left(Z_1(\omega_3)+Z_1(\omega_4)\right)-\left(\frac{t}{a}\right)Z_1(\omega_o)\right]}{1-\frac{t}{a}} \tag{9b}$$

and

$$\begin{cases}L_e=\dfrac{(X_3+X_4)}{\omega_o[2+\delta_3+\delta_4]} & \text{(inductive coupling)}\\ C_e=-\dfrac{[2+\delta_3+\delta_4]}{\omega_o(X_3+X_4)(1+\delta_3)(1+\delta_4)} & \text{(capacitive coupling).}\end{cases} \tag{9c}$$

Having obtained Q_o, ω_o, and R_o from (6a), (6b), and (9a), respectively, the resonator elements L_o and C_o can be evaluated using (4b).

Once the equivalent circuit of the high-Q resonator is established with all its elements determined, the coupling coefficient (κ) and the loaded resonant frequency (f_L) can be computed directly from the circuit by analyzing the impedances seen at port 2, as illustrated in Fig. 1. The external admittance to the left-hand side of port 2 is defined as [19]

$$Y_e=G_e+jB_e=(G_{e1}+G_{e2})+jB_e \tag{10a}$$

where

$$G_{e1}=\frac{R_s}{(R_s+R_e)^2+X_e^2}\quad G_{e2}=\frac{R_e}{(R_s+R_e)^2+X_e^2} \tag{10b}$$

and

$$B_e=\frac{-X_e}{(R_s+R_e)^2+X_e^2}. \tag{10c}$$

The total admittance (Y_T) at port 2 can thus be written as

$$\begin{aligned}Y_T&=Y_e+Y_o\\&=(G_e+G_o)+j\left[G_oQ_o\left(\frac{\omega}{\omega_o}-\frac{\omega_o}{\omega}\right)+B_e\right]\\&=(G_e+G_o)+2jG_oQ_o\xi E\end{aligned} \tag{11a}$$

where

$$\xi=\frac{\omega-\omega_L}{\omega_o}=\frac{\omega-\omega_o}{\omega_o}-\frac{\omega_L-\omega_o}{\omega_o}=\delta-\delta_L \tag{11b}$$

and

$$E=\frac{1}{2}\left[1+\frac{\omega_o}{\omega_L}(1+\delta)^{-1}\right]. \tag{11c}$$

In (11c), ω_L is the loaded resonant angular frequency at which the imaginary part of Y_T vanishes. It can be solved, leading to the original expression (12a), shown at the bottom of the following page, where Q_{se} is the source reactance quality factor given by

$$Q_{se}=\frac{|X_e(\omega_o)|}{(R_s+R_e)}=\frac{|B_e(\omega_o)|}{G_e} \tag{12b}$$

and Q_{so} is the corresponding resonator quality factor normalized to the total source resistance given by

$$\begin{aligned}Q_{so}&=\frac{\omega_oL_o}{(R_s+R_e)}\\&=\frac{1}{\omega_oC_o(R_s+R_e)}\\&=\frac{1}{G_oQ_o(R_s+R_e)}\\&=\frac{1}{(R_s+R_e)}\sqrt{\frac{L_o}{C_o}}\end{aligned} \tag{12c}$$

which are defined and used here. For the high-Q resonator, ω_L is close to ω_o and, hence, in the vicinity of the resonant frequency, $\delta \ll 1$ and parameter E in (11c) is approximately one. Therefore, (11a) can be simplified to give

$$\begin{aligned} Y_T &= (G_e + G_o) + 2jG_oQ_o\xi \\ &= (G_e + G_o)\left[1 + 2jQ_L\frac{\omega - \omega_L}{\omega_o}\right] \end{aligned} \tag{13a}$$

where the loaded quality factor of the resonator

$$Q_L = \frac{Q_o}{1+\kappa} \tag{13b}$$

and the overall coupling coefficient

$$\kappa = \frac{G_e(\omega_L)}{G_o} = \kappa_1 + \kappa_2, \tag{13c}$$

with

$$\kappa_1 = \frac{G_{e1}(\omega_L)}{G_o} \text{ and } \kappa_2 = \frac{G_{e2}(\omega_L)}{G_o}. \tag{13d}$$

Also, the input reflection coefficient at port 1 is defined as

$$\begin{aligned} \Gamma_1 &= e^{2j\beta l}\Gamma_i \\ &= \frac{R_e + jX_e + Z_o - R_s}{R_e + jX_e + Z_o + R_s} \\ &= \frac{Y_e\left[Y_o(R_e + jX_e - R_s) + 1\right]}{Y_o + Y_e}. \end{aligned} \tag{14}$$

For a high-Q resonator over a narrow band of frequency near ω_L, a detuned reflection coefficient can be defined, which is given by

$$\begin{aligned} \Gamma_d &= Y_e\left[R_e + jX_e(\omega_L) - R_s\right] \\ &= \frac{R_e + jX_e(\omega_L) - R_s}{R_e + jX_e(\omega_L) + R_s} \\ &= \rho_d e^{j\theta_d}. \end{aligned} \tag{15}$$

Substituting (15) into (14), an approximate expression for Γ_1 can be obtained such that

$$\Gamma_1 = e^{2j\beta l}\Gamma_i \approx \frac{Y_o\Gamma_d + Y_e}{Y_o + Y_e} \tag{16}$$

from which the magnitude of the input reflection coefficient at port i can be written as

$$\rho_i^2 = |\Gamma_i|^2 = |\Gamma_1|^2 = \rho_d^2 - \frac{1}{(1+\kappa)^2}\frac{p\xi + q}{r\xi + 1} \tag{17a}$$

where

$$p = 4Q_o\rho_d\Big[\kappa\big(\sin(\theta_d) - hQ_{se}\cos(\theta_d)\big) - 2Q_o\delta_L\rho_d\Big] \tag{17b}$$

$$\begin{aligned} q =& \rho_d^2\kappa(\kappa+2) - \kappa^2\left(1 + h^2Q_{se}^2\right) \\ & - 2\kappa\rho_d\big(\cos(\theta_d) - hQ_{se}\sin(\theta_d)\big) + (2Q_o\delta_L\rho_d)^2 + \delta_L p \end{aligned} \tag{17c}$$

$$r = 4Q_L^2 \tag{17d}$$

and

$$h = \begin{cases} -\left(\dfrac{\omega_L}{\omega_o}\right) \approx -1 & \text{(inductive coupling)} \\ \left(\dfrac{\omega_o}{\omega_L}\right) \approx 1 & \text{(capacitive coupling).} \end{cases} \tag{17e}$$

Thus, from (17a), a minimum of ρ^2 is expected to occur near ω_L when the second term on the right-hand side of the equation reaches its maximum at $\xi_{\min}$, which is defined as

$$\xi_{\min} = \begin{cases} \sqrt{\left(\dfrac{q}{p}\right)^2 + \dfrac{1}{r}} - \dfrac{q}{p}, & \text{if } \dfrac{q}{p} > 0 \Rightarrow \xi_{\min} > 0 \\ -\sqrt{\left(\dfrac{q}{p}\right)^2 + \dfrac{1}{r}} - \dfrac{q}{p}, & \text{if } \dfrac{q}{p} < 0 \Rightarrow \xi_{\min} < 0. \end{cases} \tag{18}$$

From (18), the relation between ω_L and $\omega_{\min}$ at which the minimum of ρ occurs, as observed on a vector network analyzer, can be easily computed. For large loaded quality factor Q_L such that $(1/r) \ll (q/p)^2$, $\xi_{\min}$ is almost zero and, hence, $\omega_{\min}$ can be approximated by ω_L. The corresponding ρ^2 at $\xi_{\min}$ is given by

$$\rho_{\min}^2 \approx \rho_d^2 - \frac{p}{8Q_o^2\xi_{\min}}. \tag{19}$$

III. Experimental and Computed Results

To illustrate the above principle and procedure, two resonators, a hollow cavity resonator, and a dielectric loaded cavity resonator were measured and their equivalent circuits were extracted separately. At first, using (1) and (2), the propagation group delay for the connecting transmission line is evaluated by the differential measurement of two connectors of different lengths. Shown in Fig. 3 is the measurement results for a length difference (Δl) of 10.5 mm when each connector was terminated in the same open load.

The average measured group delay per unit length is found to be 4.469 ps/mm, which is used in subsequent measurements for

$$\omega_L = \begin{cases} \omega_o\sqrt{\dfrac{1}{2}\left(1 + \dfrac{Q_{so}}{Q_{se}} - \dfrac{1}{Q_{se}^2}\right) + \sqrt{\dfrac{1}{4}\left(1 + \dfrac{Q_{so}}{Q_{se}} - \dfrac{1}{Q_{se}^2}\right)^2 + \dfrac{1}{Q_{se}^2}}} & \text{(inductive coupling)} \\ \omega_o\sqrt{\dfrac{1}{2}\left(1 - Q_{so}Q_{se} - Q_{se}^2\right) + \sqrt{\dfrac{1}{4}\left(1 - Q_{so}Q_{se} - Q_{se}^2\right)^2 + Q_{se}^2}} & \text{(capacitive coupling)} \end{cases} \tag{12a}$$

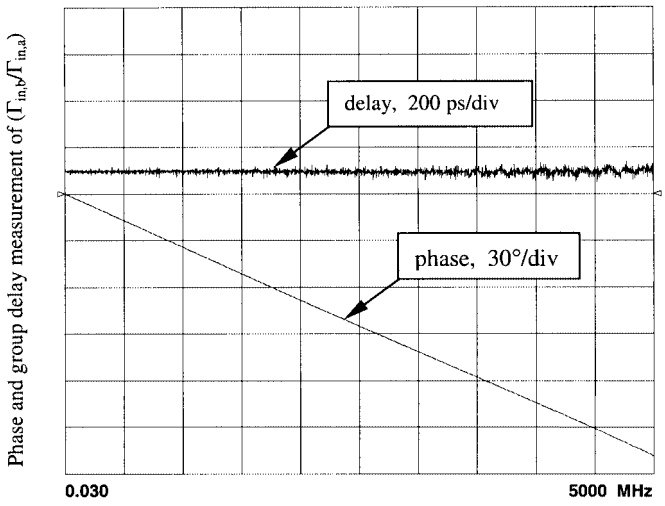

Fig. 3. One-port differential measurement of two connectors $\Gamma_{\mathrm{in,b}}/\Gamma_{\mathrm{in,a}}$ for $\Delta l = 10.50$ mm.

deembedding the delay due to the connecting transmission line of a given length when characterizing the two resonators.

The case of the hollow cavity is of over-coupled and the measurements of its input impedance are shown in Fig. 4(a) after the delay due to the connector is deembedded. The resonator is a cubic aluminum cavity with an inner side length of 50 mm. The resonant mode within the cavity is TM_{110}, excited via a probe of a subminiature A (SMA) coaxial connector placed at the centre of a sidewall at a distance of 12.02 mm up to the inner wall of the cavity. The probe has a diameter of 1.27 mm and a length of 4.0 mm penetrating into the cavity. The electrical delay due to the connector is 53.72 ps. The radius of curvature at the four corners of the inner wall of the cavity is 7.0 mm [see Fig. 4(b)]. Copper foil of 0.2-mm thickness was placed between the aluminum lid and the opening of the cavity in order to stop the electromagnetic leakage from the cavity.

For the hollow cavity, the measured frequencies at the critical and detuned crossover points and their corresponding impedances are summarized in Table I. To quantify the accuracy of the analysis presented in this paper, the Q factors, coupling coefficient, and loaded resonant frequencies computed using the present analysis are compared with those computed from the Qzero computer program developed by Kajfez [19] based on the multipoint numerical technique. Table II shows the results for both analyzes. Very good agreement between the two sets of data is observed.

During the determination of the impedances presented in Table I, it was found that a large number of points were concentrated around the detuned region when the measurement was taken with 1601 frequency points equally spaced over a span of 302 MHz on an Agilent 8753D vector network analyzer. In order to locate accurately the critical points from the measured data, a second measurement was taken around the resonant frequency with the same number of points over a narrower span of 63 MHz from 4.185 to 4.248 GHz. However, a more advanced vector network analyzer, such as Agilent 8510C [20] equipped with the frequency segmentation function, overcomes the problem of insufficient points around the resonant frequency in the first measurement.

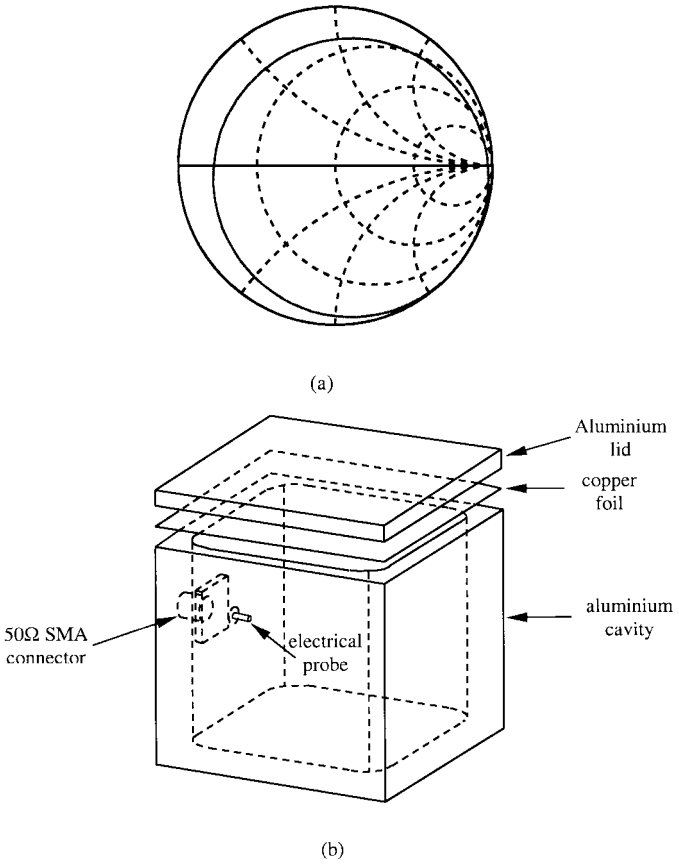

Fig. 4. (a) Deembedded impedance locus (Z_1). (b) Assembly of the overcoupled hollow cavity resonator.

TABLE I
MEASURED FREQUENCIES AT THE CRITICAL AND CROSSOVER POINTS TOGETHER WITH THE CORRESPONDING IMPEDANCES FOR THE OVERCOUPLED HOLLOW CAVITY RESONATOR IN FIG. 4(b)

Measured frequencies and corresponding impedances	
f_1 = 4.22217 GHz	$Z_1(f_1)$ = 1803.5 + j 1621.2
f_2 = 4.22280 GHz	$Z_1(f_2)$ = 1703.7 – j 1913.8
f_3 = 4.06400 GHz	$Z_1(f_3)$ = 0.20531 – j 143.67
f_4 = 4.36600 GHz	$Z_1(f_4)$ = 0.24689 – j 143.84
f_o = 4.22249 GHz	$Z_1(f_o)$ = 3522.5 – j 240.13

TABLE II
COMPARISON OF PARAMETERS OBTAINED FROM THE ANALYSIS PRESENTED IN THIS PAPER AND THOSE FROM THE Qzero COMPUTER PROGRAM BY KAJFEZ [19] FOR THE OVERCOUPLED HOLLOW CAVITY RESONATOR

Parameters	Presnet Analysis	Qzero software [20]
Q_o	6702.3	6385.0
Q_L	766.83	759.20
κ	7.6277	7.4098
f_L	4.2156 GHz	4.2134 GHz

Using the impedances in Table I in the appropriate equations in Section II, the elements of the equivalent circuit can be extracted: $R_e = 0.2108\ \Omega$, $C_e = 0.2630$ pF, $R_o = 3522.5\ \Omega$, $L_o = 19.809$ pH, and $C_o = 71.721$ pF. The corresponding calculated values of $f_{\min}$ and $\rho_{\min}$ are 4.2156 GHz and 0.7617, respectively, which are in very good agreement with the measured values $f_{\min} = 4.2155$ GHz and $\rho_{\min} = 0.7549$, shown in

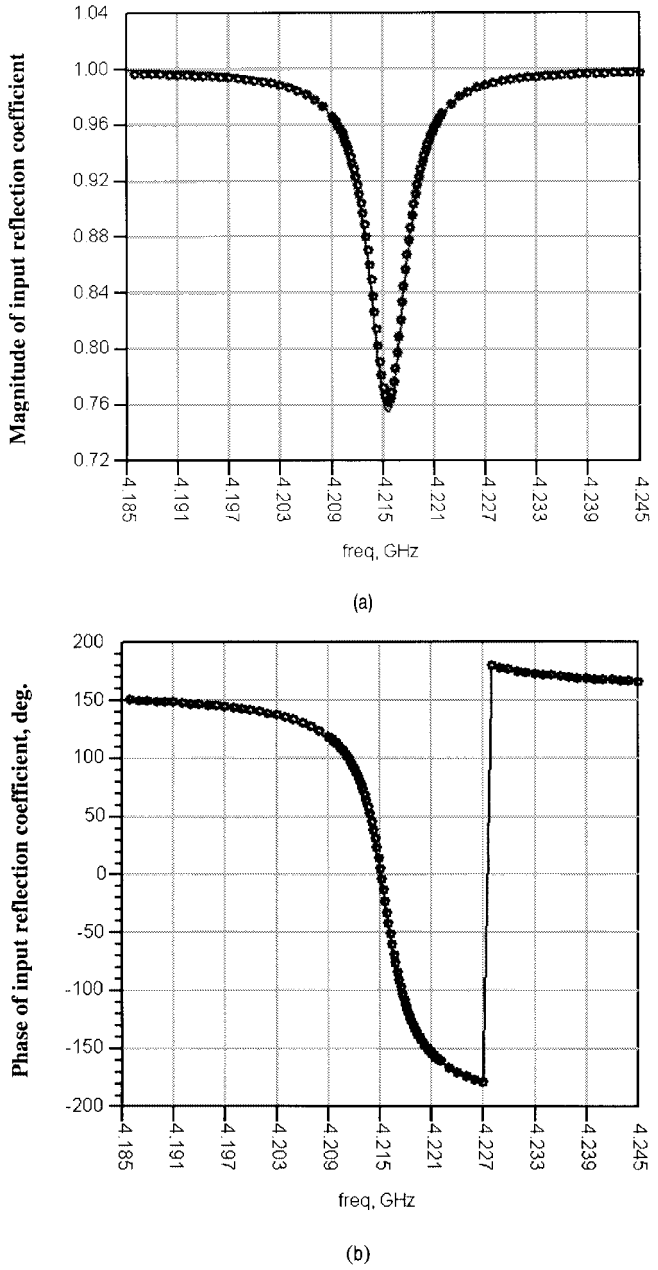

Fig. 5. Comparison between the measured response (—) and the ADS computed response (•) for: (a) magnitude and (b) phase for the overcoupled hollow cavity resonator including the delay due to the connector.

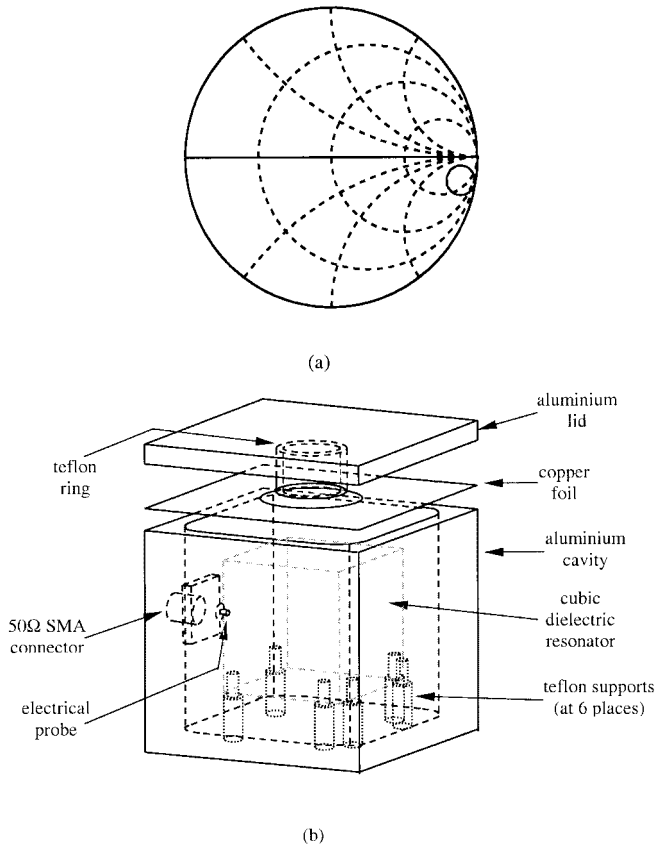

Fig. 6. (a) Deembedded impedance locus (Z_1). (b) Assembly of the undercoupled dielectric loaded cavity resonator.

TABLE III
MEASURED FREQUENCIES AT THE CRITICAL AND CROSSOVER POINTS TOGETHER WITH THE CORRESPONDING IMPDEDANCES OF THE UNDERCOUPLED DIELECTRIC LOADED CAVITY RESONATOR

Measured frequencies and corresponding impedances	
f_1 = 1.7950475 GHz	$Z_1(f_1)$ = 369.16 – j 206.36
f_2 = 1.7951675 GHz	$Z_1(f_2)$ = 365.89 – j 912.89
f_3 = 1.7756125 GHz	$Z_1(f_3)$ = 7.8368 – j 575.66
f_4 = 1.8020000 GHz	$Z_1(f_4)$ = 7.8979 – j 575.73
f_o = 1.7951075 GHz	$Z_1(f_o)$ = 717.45 – j 570.86

Fig. 5. Note that the delay due to the connector is included in the results in Fig. 5. To support the high accuracy of the extracted circuit elements, the ADS simulation of the phases and magnitudes using the extracted elements are also presented in Fig. 5, which are almost indistinguishable from the measured ones.

In another example, a dielectric loaded cavity resonator in the undercoupled condition is measured and the result is shown in Fig. 6(a). Again the delay (53.72 ps, as in first example) due to the connector is deembedded. As illustrated in Fig. 6(b), the resonator is an aluminum cubic cavity with a side of 45 mm, loaded concentrically with a dielectric cube of a side 29.4 mm supported by Teflon posts. Like the previous resonator, the radius of curvature at the four corners of the cavity is 7.0 mm. A Teflon ring of an inner diameter of 17.0 mm with a thickness of 1.5 mm and a height of 8.8 mm is mounted onto a 1-mm-deep groove on the aluminum lid. This will help to hold the dielectric resonator at the center of the aluminum cavity when the cavity is closed with the lid. Copper foil of 0.2-mm thickness is placed between the opening of the cavity and the lid to act as an electromagnetic choke. The resonant mode within the cavity is $TM_{11\delta}$ excited via a probe of an SMA coaxial connector placed at the center of a sidewall at a length of 12.02 mm up to the inner wall of the cavity. The probe penetrating into the cavity has a diameter equal to 1.27 mm and a length equal to 1.0 mm.

For the dielectric loaded resonator, the measured frequencies at the critical and detuned crossover points and their corresponding impedances are presented in Table III. The accuracy of the technique presented in this paper for obtaining the Q factors, coupling coefficient, and loaded resonant frequencies is checked against those computed by the Qzero computer

TABLE IV
COMPARISON OF PARAMETERS OBTAINED FROM THE ANALYSIS PRESENTED IN THIS PAPER AND THOSE FROM THE Qzero PROGRAM BY KAJFEZ [19] FOR THE UNDERCOUPLED DIELECTRIC LOADED CAVITY RESONATOR

Parameters	Results from Analysis	Results from Qzero
Q_o	14959	14924
Q_L	13325	13452
κ	0.12263	0.10950
f_L	1.795034 GHz	1.795035 GHz

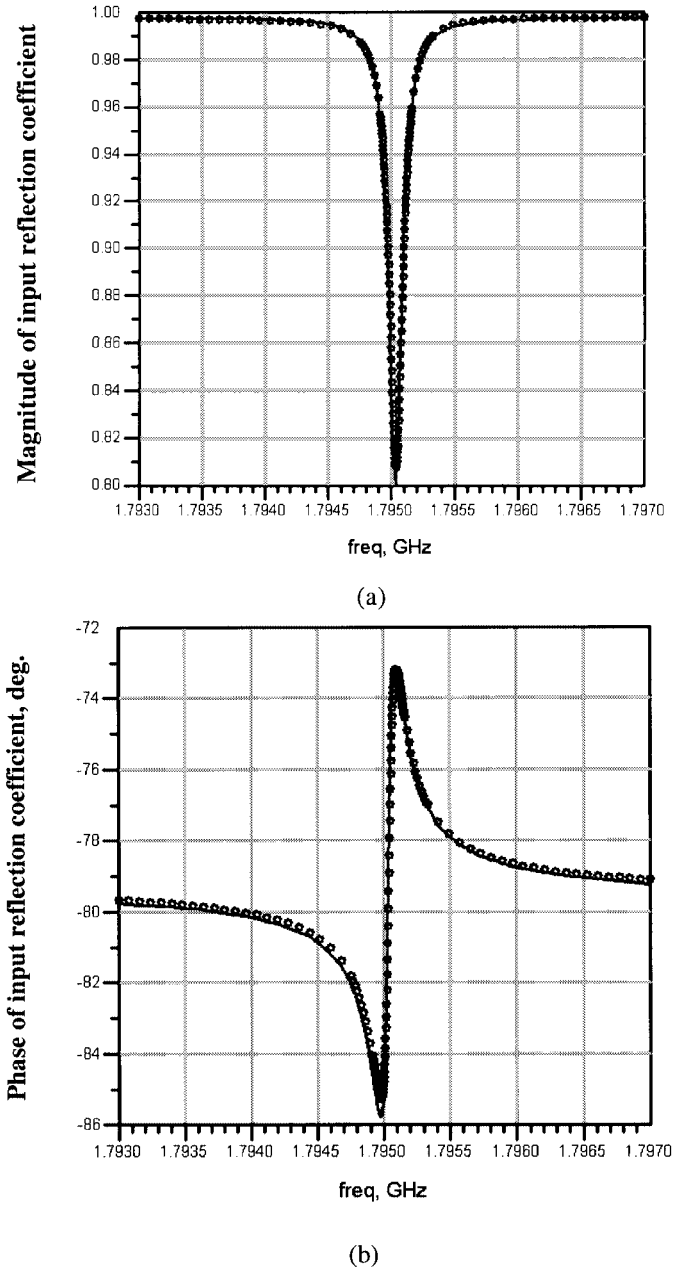

Fig. 7. Comparison between the measured response (—) and the ADS computed response (•) for: (a) magnitude and (b) phase of the undercoupled dielectric loaded cavity resonator including the delay due to the connector.

program developed by Kajfez [19] based on the multipoint numerical technique. Table IV shows the results for both analyses. As in the previous case, there is very good agreement between the two sets of results.

Using the impedances in the appropriate equations in Section II, the extracted elements of the equivalent circuit for the undercoupled dielectric loaded cavity resonator are $R_e = 7.8527\ \Omega$, $C_e = 0.15455$ pF, $R_o = 709.60\ \Omega$, $L_o = 4.2058$ pH, and $C_o = 1.8690$ nF. The corresponding calculated values of $f_{\min}$ is 1.795035 GHz and $\rho_{\min}$ is 0.8089, which is in good agreement with the measured values of $f_{\min} = 1.795030$ GHz and $\rho_{\min} = 0.8000$, shown in Fig. 7. Fig. 7 also includes the results of the ADS simulation (computed) of phases and magnitudes when the extracted elements are used in the simulations. As this figure shows, there is little difference between the measured and simulated values, confirming the high accuracy of the extracted elements.

IV. CONCLUSION

A systematic approach to the full characterization of high-Q resonators based on a one-port measurement technique has been presented. The method extends the previously established critical-points methods of unloaded Q-factor measurement. With the additional knowledge of the impedances at specific points on the impedance locus of the deembedded measured input reflection coefficient of the resonator, all lumped elements associated with the resonator equivalent circuit can be extracted and computed directly without any numerical optimization. An original expression for the loaded resonant frequency of the resonator is also given and an approximate relation between f_L and $f_{\min}$ at which the minimum magnitude of the input reflection coefficient occurs is also derived. For a very high unloaded Q factor, this measured $f_{\min}$, as observed on the network analyzer, could be taken as f_L in most practical cases. With the aid of two examples, a hollow cavity resonator and a dielectric loaded cavity resonator, the principle and procedure outlined in this paper were demonstrated. Excellent agreement between the measured and computed results were observed for both overcoupling and undercoupling conditions, thus confirming the usefulness of the method.

REFERENCES

[1] E. L. Ginzton, "Microwave Q measurements in the presence of coupling losses," *Trans. IRE Microwave Theory Tech.*, vol. MTT-6, pp. 383–389, Oct. 1958.
[2] A. Podcameni, L. F. M. Conrado, and M. M. Mosso, "Unloaded quality factor measurement for MIC dielectric resonator application," *Electron. Lett.*, vol. 17, no. 18, pp. 656–658, Sept. 1981.
[3] A. Kahnna and Y. Garault, "Determination of loaded, unloaded and external quality factors of a dielectric resonator coupled to a microstrip line," *IEEE Trans. Microwave Theory Tech.*, vol. MTT-31, pp. 261–264, Mar. 1983.
[4] D. Kajfez and E. Hwan, "Q-factor measurement with network analyzer," *IEEE Trans. Microwave Theory Tech.*, vol. MTT-32, pp. 666–670, July 1984.
[5] W. P. Wheless and D. Kajfez, "Experimental characterization of multimoded microwave resonators using automated network analyzer," *IEEE Trans. Microwave Theory Tech.*, vol. MTT-35, pp. 1263–1270, Dec. 1987.
[6] K. D. McKinstry and C. E. Patton, "Method for determination of microwave cavity quality factors from equivalent electronics circuit models," *Rev. Sci. Instrum.*, vol. 60, no. 3, pp. 439–443, Mar. 1989.
[7] M. C. Sanchez, E. Martin, and J. Zamarro, "New vectorial automatic technique for characterization of resonators," *Proc. Inst. Elect. Eng.*, pt. H, vol. 136, pp. 147–150, Apr. 1989.

[8] ——, "Unified and simplified treatment of techniques for characterising transmission, reflection or absorption resonators," *Proc. Inst. Elect. Eng.*, pt. H, vol. 137, pp. 209–212, Aug. 1990.
[9] D. Kajfez, "Q-factor measurement with a scalar network analyzer," *Proc. Inst. Elect. Eng.*, pt. H, vol. 142, no. 5, pp. 369–372, Oct. 1995.
[10] R. S. Kwok and J. F. Liang, "Characterization of high-Q resonators for microwave-filter applications," *IEEE Trans. Microwave Theory Tech.*, vol. 47, pp. 111–114, Jan. 1999.
[11] E. Y. Sun and S. H. Chao, "Unloaded Q measurement – The critical-points method," *IEEE Trans. Microwave Theory Tech.*, vol. 43, pp. 1983–1986, Aug. 1995.
[12] D. H. Han and Y. S. Kim, "Two port cavity Q measurement using scattering parameters," *Rev. Sci. Instrum.*, vol. 67, no. 6, pp. 2179–2181, June 1996.
[13] K. Leong, J. Mazierska, and J. Krupka, "Measurements of unloaded Q-factor of transmission mode dielectric resonators," in *IEEE MTT-S Int. Microwave Symp. Dig.*, Denver, CO, June 8–14, 1997, pp. 1639–1646.
[14] K. Leong and J. Mazierska, "Accurate measurements of surface resistance of HTS films using a novel transmission mode Q-factor technique," *J. Superconduct.*, vol. 14, no. 1, pp. 93–103, 2001.
[15] D. Kajfez, S. Chebolu, M. R. Abdul-Gaffoor, and A. A. Kishk, "Uncertainty analysis of the transmission-type measurement of Q-factor," *IEEE Trans. Microwave Theory Tech.*, vol. -47, pp. 367–371, Mar. 1999.
[16] I. Awai, A. C. Kundu, and T. Yamashita, "Equivalent-circuit representation and explanation of attenuation poles of a dual-mode dielectric-resonator bandpass filter," *IEEE Trans. Microwave Theory Tech.*, vol. 46, pp. 2159–2163, Dec. 1998.
[17] P. Harscher and R. Vahldieck, "Automated computer-controlled tuning of waveguide filters using adaptive network models," *IEEE Trans. Microwave Theory Tech.*, vol. 49, pp. 2125–2130, Nov. 2001.
[18] P. Harscher, R. Vahldieck, and A. Amari, "Automated filter tuning using generalized low-pass prototype networks and gradient-based parameter extraction," *IEEE Trans. Microwave Theory Tech.*, vol. 49, pp. 2532–2538, Dec. 2001.
[19] D. Kajfez, *Q Factor*. Oxford, MS: Vector Fields, 1994.
[20] *8510C Vector Network Analyzer User's Guide*, Agilent Technol., Palo Alto, CA, pp. 4.69–4.72.

Lye Heng Chua (S'00) received the B.Eng. (with honors) and M.Eng. degrees in microwaves from the National University of Singapore, Singapore, in 1987 and 1995, respectively, and is currently working toward the Ph.D. degree in electronic systems engineering at the University of Essex, Colchester, U.K.

Prior to joining the University of Essex in October 2000, he was involved in the microwave industry for over ten years. From 1987 to 1997, he was with the defence and commercial industry in Singapore, where he was involved with microwave components and circuits for system applications. From 1997 to 2000, he was a Research Associate with the Microelectronics Centre, School of Electrical and Electronic Engineering, Nanyang Technological University of Singapore, where he focused on monolithic microwave integrated circuit (MMIC) design. His research interests include microwave device modeling, filters, microwave and millimeter-wave planar structure analysis, and MMIC design.

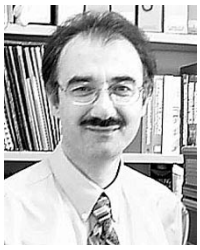

Dariush Mirshekar-Syahkal (SM'93) received the B.Sc. degree (with distinction) in electrical engineering from Tehran University, Tehran, Iran, in 1974, and the M.Sc. degree in microwaves and modern optics and Ph.D. degree from the University College London, University of London, London, U.K., in 1975 and 1979, respectively.

From 1979 to 1984, he conducted research in the characterization of millimeter-band planar transmission lines and nondestructive evaluation of metals by electromagnetic techniques at the University College London. Since 1984, he has been with the University of Essex, Colchester, U.K., where he is currently a Professor and the Head of the RF Engineering and Propagation Research Group, Department of Electronic Systems Engineering. His current research concerns problems of electromagnetic theory associated with microwave planar structures, including planar antennas, design of compact dielectric and conductor loaded cavity filters, and characterization of flaws in metals. He has authored numerous technical publications including *Spectral Domain Method for Microwave Integrated Circuits* (New York: Wiley, 1990).

Dr. Mirshekar-Syahkal is a Chartered Engineer in the U.K. He is a Fellow of the Institution of Electrical Engineers (IEE), U.K.